



GHGT-9

Wellbore integrity analysis of a natural CO₂ producer

Walter Crow^a, D. Brian Williams^a, J. William Carey^b, Michael Celia^c, Sarah Gasda^d *

^aBP Alternative Energy, 501 Westlake Park Blvd., Houston Texas, 77079, USA

^bLos Alamos National Laboratory, Los Alamos, New Mexico 87545, USA

^cPrinceton University, Princeton, New Jersey, 08544

^dUniversity of North Carolina, Chapel Hill, North Carolina, 27514, USA

Abstract

The long-term integrity of wellbores in a CO₂-rich environment is a complex function of material properties and reservoir conditions including brine and rock compositions, CO₂ pressure, and formation pressure and temperature gradients. Laboratory experiments can provide essential information on rates of material reaction with CO₂. However, field data are essential for assessing the integrated effect of these factors in subsurface conditions to provide a basis for validation of numerical models of wellbore behavior.

We present a comprehensive study and conclusions from an investigation of a 30-year old well from a natural CO₂ production reservoir. The wellbore was exposed to a 96% CO₂ fluid from the time of cement placement. This site is unique for two reasons: it represents a higher, sustained concentration of CO₂ compared to enhanced oil recovery fields and both the reservoir and caprock are clastic rocks that may possess less buffering capacity than carbonate reservoirs.

A sampling program resulted in the recovery of 10 side-wall cement cores extending from the reservoir through the caprock. The hydrologic, mineralogical and mechanical properties of these samples were measured and those results were combined with an in-situ pressure-response test to investigate cement integrity over a range of length scales. Fluid sampling was conducted with pressure and temperature measurements for geochemical analysis of the cemented annulus and the adjacent formation. These combined data sets provide an assessment of well integrity including original cement seal and the impacts of CO₂. Cement evaluation wireline surveys indicate good coverage and bonding, consistent with observations from sidewall cement core samples that have tight interfaces with the casing and formation. Although alteration of the cement samples is present in all cores in varying degrees, hydraulic isolation has prevented leakage based on the pressure gradient measured between the caprock and CO₂ formation as well as lack of corrosion and no casing pressure history. Simulation of a hydraulic isolation test (Vertical Interference Test) indicates the best match for effective permeability of the wellbore system is approximately 1-10 millidarcies which suggests cement interfaces are a more significant potential migration pathway as compared with the cement matrix. Effective placement of the Portland-fly ash cement system was a key element in the observed performance of the barrier system that provides hydraulic isolation. The types of information collected in this survey permit analysis of individual components (casing, cement and reservoir fluid and pressure measurements) for comparison to the larger scale system including the interfaces. The results will be used as part of the CO₂ Capture Project's effort to develop a long-term predictive simulation tool to assess wellbore integrity performance in CO₂ storage sites.

© 2009 BP Alternative Energy. Published by Elsevier Ltd. All rights reserved

Keywords: CO₂ Storage; well integrity; cement barrier; cement capillary pressure; effective permeability; vertical interference test; cement mineralogy

* Corresponding author. Tel.: +1-281-366-3801; fax: +1-281-504-2244.
E-mail address: walter.crow@bp.com.

1. Introduction: Well Construction and History

A field study of a 30-year old well from a natural CO₂ reservoir was conducted to determine the effect of CO₂ on the well barrier system defined as the tubulars and cement including its contact with casing and the formation. When CO₂ combines with moisture in the reservoir, carbonic acid is created which may corrode metal and Portland cement used in well construction. Fluid samples, cores and pressure response data were collected and analyzed to determine the potential effect of CO₂ on the barrier system. This information is used to provide benchmark data for modeling of the long term effects of injected CO₂ on the well system.

The field survey was conducted in a well completed in the Dakota Sandstone formation found at 4561' True Vertical Depth (TVD) and had an estimated original reservoir pressure of 1624 psi and temperature of 136 °F at that datum. The CO₂ in the reservoir is a supercritical phase under those conditions. This zone produces 96% CO₂ and has an average permeability of 59 millidarcies (mD), with a mineralogy that includes 69% quartz, less than 10% carbonate and water saturation of 20% based on original drill core analysis from this interval. The caprock confining layers in this well that overlie the Dakota formation are the Graneros Shale (135' vertical thickness) and Greenhorn Shale/Limestone (75' vertical thickness) formations (Figure 1.1).

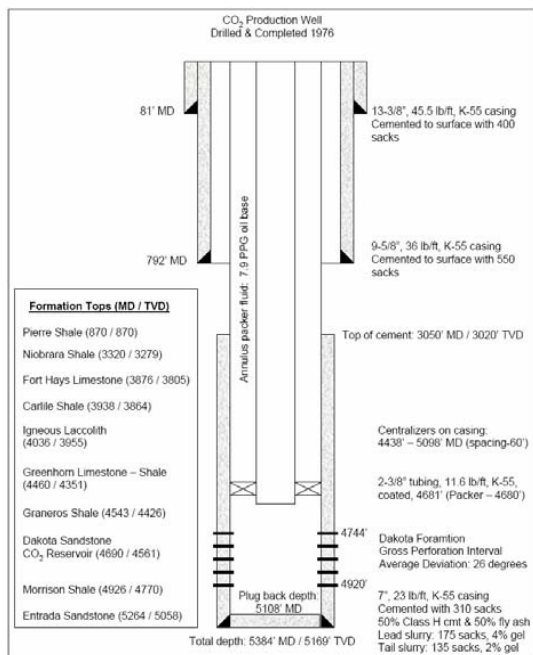


Figure 1.1: Schematic diagram outlining the type, size and grade of tubulars used in the well construction. Production tubing was plastic-coated carbon steel and cement was a Portland cement system with 50% fly ash.

2. Sample analysis

Solid and fluid samples were collected from outside the casing within the CO₂ reservoir and from the caprock shale. Sidewall cores were cut through the casing to recover casing, cement and formation samples. Cement samples were analyzed for permeability, porosity, capillary pressure properties, formation factor and Young's Modulus (Fig 2.1). Cement cores taken near the CO₂ reservoir have higher average permeability (21 μD) and porosity (41%) compared to cores collected near the top of the caprock of 1 μD permeability and 25% porosity. Cement core mineralogy (Figure 2.2) determined by X-ray diffraction indicates the relative amount of original unaltered cement paste compared to the amount converted to calcium carbonate due to CO₂ exposure over the life of the well. Cement samples taken in and near the CO₂ reservoir have been almost completely converted to calcium carbonate. Samples at the top of the caprock retain more of the original cement mineralogy but have had some minimal alteration. Cement evaluation log information given by raw acoustic impedance (Fig 2.1) indicates generally good cement quality with the highest quality near the top of the shale at 4500' MD (shown by the darker brown color in the log strip). Visual observation of the cement interfaces with casing

The well was drilled in 1976 but production was deferred 9 years until 1985 due to pipeline availability. The well produced a total of 20 years and the first 13 years averaged 7000 standard cubic feet per day (SCF/D) of CO₂ with associated water production of 0.75 barrel per 1000 SCF. The final 7 years of production was intermittent due to increased water production. Produced water from this interval is less than 5000 parts per million total dissolved solids (TDS). There was no casing pressure observed over the 30 year life of the well. Produced water samples from the central facility indicate a range of pH 3.1 to 6.0 in recent years. The well was drilled with an oil-based mud and the barrier system consisted of 7-inch diameter casing cemented with a Portland-cement-fly ash system. The casing was carbon steel, K-55 grade and was centralized in the borehole. The cement was 310 sacks (391 ft³) of Class H Portland cement with 50% fly ash, 3% bentonite gel mixed at a density of 14.2 pounds per gallon (specific gravity: 1.71). The top of the cement (behind casing) was 3050' measured depth (MD) which extended 1640' above the CO₂-bearing reservoir. The casing was pressure tested to 1000 psi for 30 minutes after a 24 hour waiting period when the estimated cement compressive strength was 2000 psi. Production tubing was plastic-coated, K-55 grade material that showed no signs of corrosion during its production life.

and with caprock show apparently tight contacts with no debris or other indications of porosity (Figs 2.3 and 2.4) and only very thin deposits (< 0.1 mm) of calcium carbonate (Fig 2.5). All 20 carbon steel casing samples recovered were in excellent condition with limited corrosion. Fluid samples were collected with a test tool that isolated formation pressure from the wellbore, drilled a hole through the casing, collected a fluid sample and recorded formation pressure and temperature data (Fig 2.1). The fluids had a surface-measured pH range of 5.2 to 6.1 and are slightly acidic. The measured formation pressure suggest that wellbore system provides hydraulic isolation between the CO₂ production zone and the upper caprock intervals based on the 1000 psi pressure difference sustained across the shale.

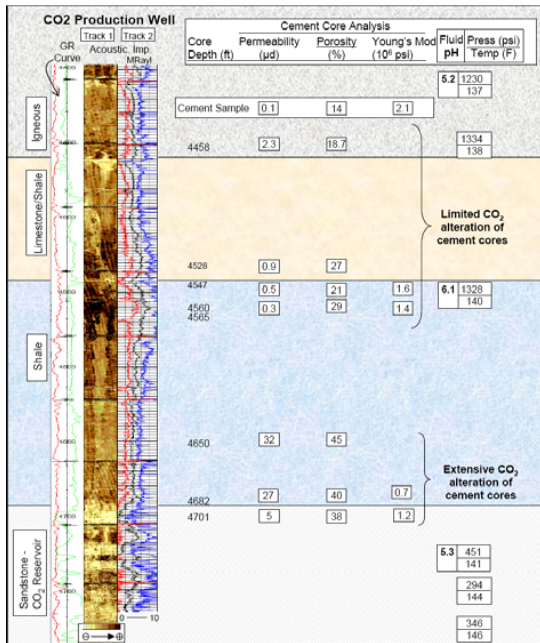


Figure 2.1: Comparison of cement core petrophysical properties with well log data, pressure data and fluid pH. Raw Acoustic Impedance map from the Ultrasonic Imaging Tool provides qualitative reference of cement condition (darker = better casing-cement bond).



Figure 2.3: Core from 4682' of cement (left) and formation (right) indicates a tight fit at the interface.



Figure 2.4: Core from 4650' with an intact contact between casing and cement.

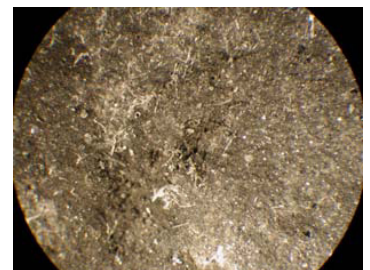


Figure 2.5: Core from 4722' in contact with the CO₂ formation has a thin layer of calcium carbonate crystals (view is 4 mm in width).

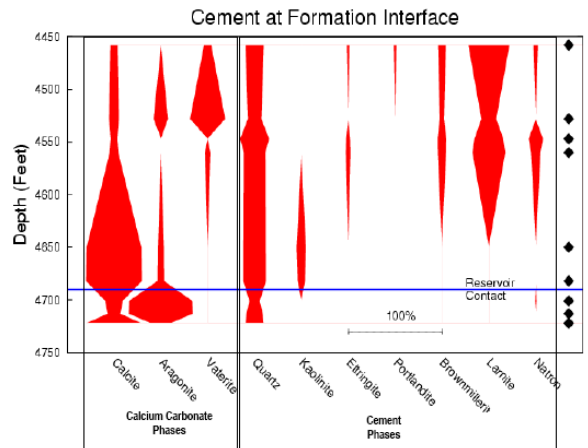


Figure 2.2: Mineralogy of cement cores measured at the interface with the formation as a function of depth. Original cement phases on the right are compared with CO₂ induced alteration to calcium carbonate phases. The amount of calcium carbonate is greatest within and near the CO₂ reservoir and original cement phases are more abundant further from the reservoir. Aragonite is the most common calcium carbonate within the reservoir; calcite is common in the region just above the reservoir contact and vaterite is limited to regions far from the reservoir.

Capillary Pressure Measurements

The capillary pressure properties of the cement cores were analyzed by centrifuge to determine the resistance to displacement of brine by air under differential pressure up to 300 psi. The estimated total pressure differential drive at the wellbore is approximately 147 psi (CO_2 buoyancy + non-hydrostatic gradient) which indicates that the capillary pressure measurements cover the expected range experienced by this wellbore system.

The capillary pressure measurements are summarized in Figure 2.3 and compared to a laboratory sample of cement prepared according to the original wellbore specifications and cured under reservoir conditions. The capillary resistance is so high for fresh, unaltered cement that air entry is not possible at pressures higher than 200 psi. These results suggest that for fresh cement, CO_2 penetration of the cement matrix would not occur and that diffusion is the only mechanism for CO_2 migration through the cement matrix which is extremely slow. By contrast, the relatively unaltered cement cores collected far from the CO_2 reservoir (shown in blue in Figure 2.3) showed that only about 5% of the available pore space was accessible at pressures > 50 psi and < 300 psi. The effect of more complete carbonation as shown in samples collected from within and near the CO_2 reservoir further reduces the capillary resistance such that about 25% of the available pore space was accessible at pressures > 50 psi and < 300 psi. Interestingly, complete carbonation produces on average a small increase in capillary entry pressure resistance over the relatively unaltered samples.

Years of downhole aging may have led to the difference in capillary pressure between laboratory samples and relatively unaltered cement samples. Our hypothesis is that for fresh cement, migration of CO_2 in the wellbore can only occur by passing through a defect in the barrier system (channel or cement interface transmission pathway) and thus alteration of the cement could only occur by diffusion of CO_2 from the defect into the cement matrix. However, it is also possible that with aging of the cement, the capillary resistance decreases and a limited volume (5%) of the available pore space could be accessible by CO_2 . In this case, CO_2 could invade a limited amount of the pore space if the entry pressure exceeded 50 psi. Alteration could then occur by diffusion from the 5% pore space occupied by CO_2 . Once the cement has been carbonated, however, it still retains relatively high capillary resistance to CO_2 . In summary, the capillary pressure measurements suggest that separate phase CO_2 migration through the cement matrix is unlikely at the pressure conditions for the wellbore.

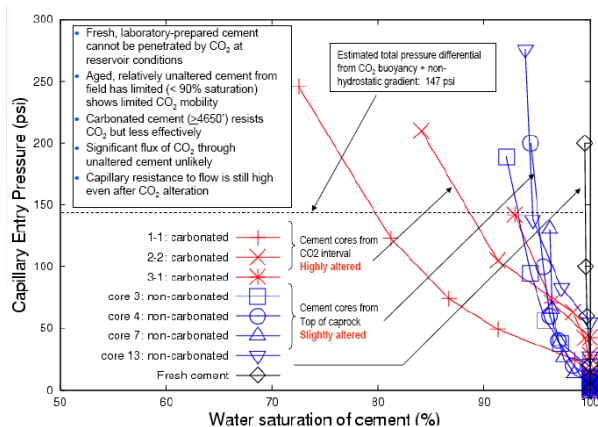


Figure 2.3: Capillary pressure properties of seven cores and a laboratory prepared cement sample. The fresh cement (black curve) shows great capillary resistance such that no displacement of brine was possible at air pressures < 200 psi. An estimated pressure differential at the caprock-reservoir contact of 147 psi (dashed line) limits capillary displacement of brine to 20% of pore space for the most carbonated cores (red curves) and to 5% for the slightly altered cores near the top of caprock (blue curves).

3. Log Analysis

The Ultrasonic Imaging Tool (USIT) was run to provide an indication of the cement quality and its bond to the casing measured by attenuation of the acoustic signal. Log results are presented in Tracks 1 and 2 in Figure 2.1. Acoustic impedance decreases from the top of the shale to the CO_2 interval (Track 2) from 8 to 0 MRayl over the interval from 4560' to 4700'. This general trend is consistent with a decrease in cement core hydrologic properties from the top of the caprock ($1\mu\text{D}$ permeability, 25% porosity) to the CO_2 interval ($21\mu\text{D}$ permeability, 41% porosity). For this well, the USIT log measurement is relatively capable of detecting differences in the quality of the cement that is attached to, and surrounding the casing (Figure 2.1).

Acoustic impedance values were plotted as a function of porosity determined on cement side-wall cores (Fig 3.2) and indicate a correlation between the log response and degree of cement core carbonation which has affected the hydrologic properties. This

suggests that acoustic impedance can point to gross changes in porosity and can be correlated with significant cement alteration in this well.

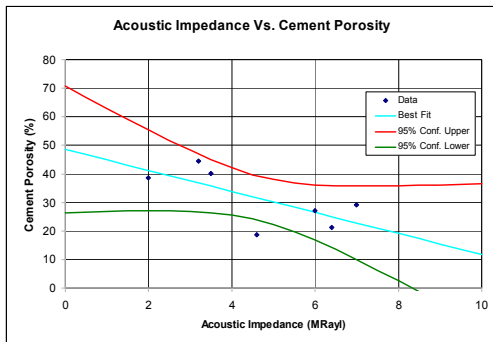


Figure 3.2: Measured cement core porosity is plotted against acoustic impedance log values from the depth that each core was collected. There is a general trend that suggests acoustic impedance is correlated with changes in porosity.

A multi-arm mechanical calliper was used to inspect the inner casing diameter and indicated minimal wall thickness loss between the perforations and packer where the casing was exposed to CO₂ and produced water. The corrosion log data is consistent with actual casing samples collected with the coring tool and showed limited or no corrosion.

There was no gas saturation evident in the caprock or other overlying layers based on results of a pulsed neutron log. This indicates no migration along the barrier system. All gas shows from the survey are within the CO₂ formation and are consistent with presence of gas from the completion.

4. Vertical Interference Test Analysis

A Vertical Interference Test (VIT) was conducted at the interface of the Greenhorn Limestone/Shale and the Graneros Shale between two perforated intervals at 4522' and 4533'. A wireline tool isolates the lower perforated interval from applied casing pressure. The applied pressure from the surface passes through the casing wall at the upper perforated zone to the cement barrier and shale interval. The pressure signal is recorded by the upper strain gauge (MRPS) and the lower quartz gauge (MRPA) adjacent to each perforation interval. The results from this test indicate the extent of hydraulic communication along the exterior of the well casing between the two perforations and are a measure of the effective permeability of the barrier system. Here, the barrier system is defined as the region outside of the casing that includes the following components: the cement that was placed between the casing and the shale (wellbore), the zone of shale that may have been damaged by drilling, and any annuli (interfaces) that may exist between the cement and the casing or the cement and the shale. The effective permeability of this system is a bulk measure of permeability but does not distinguish individual flowpaths within the different components of the barrier system. Therefore, effective permeability is an integrated measure of the overall competence of the barrier system to prevent fluid and gas migration along the wellbore.

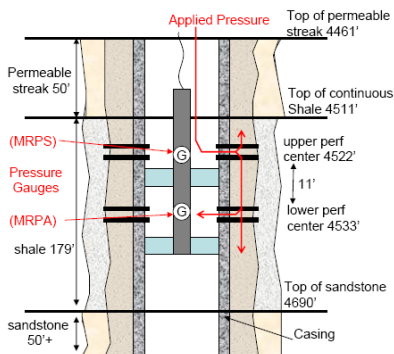


Figure 4.1: Configuration of VIT includes an isolation tool with pressure gauges (MRPS & MRPA) positioned in the

wellbore. The model describes perforations in a shale interval with sand (permeable) intervals above and below the shale.

The approach taken in the VIT analysis is to use a numerical model developed for this analysis to simulate the physical test data. The effective permeability assigned to this region in the model is then tuned until the simulated data sufficiently matches the test data. This approach requires that other system parameters can be reasonably estimated, which include the permeability and compressibility of the shale and other geologic formations within the domain, the compressibility of cement, and the effective permeability of other sections of barrier system along the wellbore.

The raw VIT data (shown in Figure 4.2) were normalized to a dimensionless scale between 0 and 1. On this scale, a value of 1 means that 100% of the pressure change imposed in the upper perforation is detected in the lower perforation. Likewise, a value of 0 means that no pressure change is detected in the lower perforation. This normalization is achieved by taking the ratio of the relative pressure changes recorded in the lower and upper gauges using Equation (4.1). An initial pressure ($MRPA_0$) of 1940 psi is used, which is the value recorded in the lower perforation at 5,600 seconds that corresponds to the wellbore fluid hydrostatic pressure (equivalent to a gradient of 0.439 psi/ft at 4417' TVD). Similarly, the relative pressure change in the upper perforation is the average sustained pressure (2725 psi) minus $MRPA_0$. Since the perforations are so close together, this is an appropriate approximation. The normalization formula is as follows:

$$MRPA_{norm} = \frac{MRPA(t) - MRPA_0}{2725 - MRPA_0} \tag{Equation 4.1}$$

Governing Equation

The governing equation for this system is the continuity equation for compressible flow of a single fluid in porous media,

$$c_f \frac{\partial p}{\partial t} - \nabla \cdot \frac{k}{\mu} (\nabla p - \rho \mathbf{g}) = 0. \tag{Equation 4.2}$$

In the above equation, c_f is the compressibility, p is the fluid pressure, k is the permeability, μ is the fluid viscosity, ρ is the fluid density, and \mathbf{g} is the gravity vector. Equation (4.2) is a transient equation that describes the evolution of pressure in space and time. For this model, compressibility and permeability can vary, but the fluid viscosity and density are assumed to be constant in the near-well environment. In Equation (4.2), the pressure response depends on the ratio k/c_f (permeability to compressibility) at each point in space. A set of values is chosen for k and c_f at each point in space. Thus, although the focus of the modelling is on permeability, the dependency on compressibility is implied.

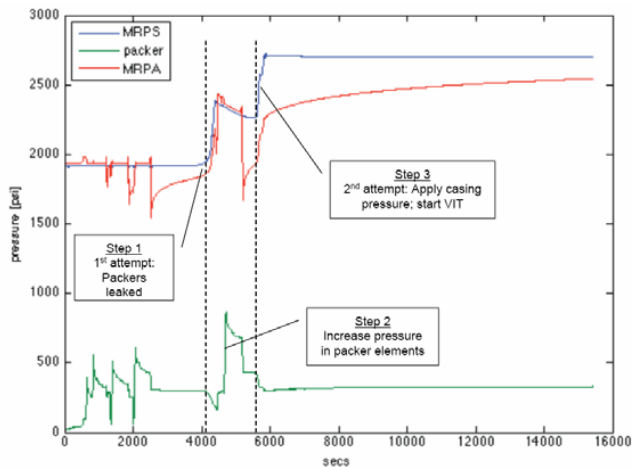


Figure 4.2: Raw data from VIT showing pressure in three gauges, MRPS in the upper perforation, MRPA in the lower perforation and the packer inflation pressure. There are two attempts to pressurize the well. The first attempt began at 4,500 s and failed due to leakage around the packers. The second attempt to pressurize began at 5,600 s and continues until the end of the test at around 15,000 s.

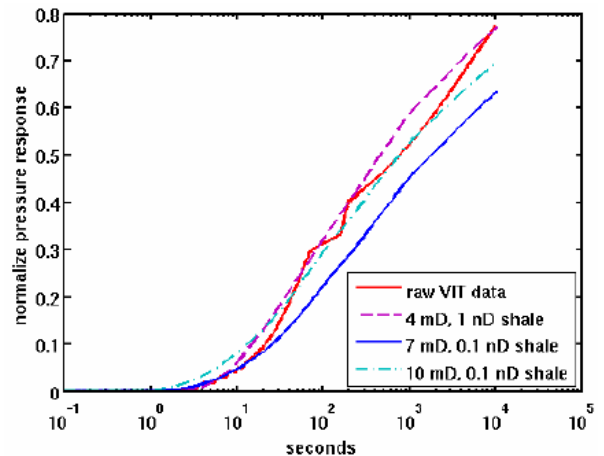


Figure 4.3: Comparison of IT data (red line) to numerical simulations under differing assumptions of cement permeability (4-10 mD) and shale permeability (0.1-1 nD).

Numerical Method

A numerical model was developed that solves the governing equations for compressible flow of a single fluid in porous media in space and time. This model solves the system in a radially symmetric coordinate system. As in the physical system, the domain that is modeled consists of two sandstone formations separated by a low-permeability shale layer. The model domain measures 256' in the vertical and 27,000' in the radial direction. The inner boundary of the domain coincides with the outer casing radius (OD) and is impermeable to flow. At the outer boundary, a hydrostatic pressure condition is imposed. The top and bottom boundaries of the domain are also impervious to flow. The perforations are modeled as very high permeability regions at the same location within the shale as in the physical system. Pressure is imposed in the upper perforation to a value of 2725 psi, which is the average applied pressure measured by the MRPA gauge in the physical system. During the VIT simulation, the pressure was recorded in the lower perf for 10,000 s and compared with the actual VIT data.

Based on original drill core measurement, the horizontal permeability value of the sandstone formations are estimated to be 0.1 D (1 Darcy = 10^{-12} m²) and are assumed to be isotropic. The permeability of the shale is assumed to be anisotropic and estimated to be 0.1 nD (horizontally) and 0.0001 nD (vertically) where 1 nD = 10^{-18} D. Based on survey sidewall core measurement, the compressibility of the sandstone is estimated to be 10^{-10} m²/N, while the shale compressibility is assumed to be higher and is estimated to be 10^{-9} m²/N. For reference, the compressibility of water is 4.6×10^{-10} m²/N, where 1 m²/N = 1 Pa⁻¹ = 6,895 psi.

The distance from the outer radius of the casing to the inner wall of the borehole is 1.75 in. This region corresponds to the barrier system as discussed above, where it is assumed that the shale outside this zone is undamaged. Determining the effective permeability of this 1.75 in wide zone is the objective of this analysis, and the value can be tuned in the model until a sufficient match is found to the test data.

Method of analysis

Using the model, numerical simulations were performed using different values of effective permeability assigned to the barrier system. After testing numerous values, the comparison with the VIT data was best for a limited number of cases. Three representative cases are discussed here. The values of the assigned effective permeability and the horizontal permeability in the shale for each case are listed in Table 4.1:

Case	Effective Permeability	Shale horizontal permeability
1	7 mD	0.1 nD
2	10 mD	0.1 nD
3	4 mD	1 nD

Table 4.1: Simulation cases that present the best matches to test data using variation of barrier system effective permeability with shale permeability

Results

The simulated VIT results for all cases are compared with the actual VIT test data (Fig. 4.3). For all the following cases, the temporal dimension is presented in log-space so as to examine both the early time and late time comparisons between the simulated and test data. In addition, the temporal values of the test data are scaled so that time $t = 0$ corresponds to the start of the VIT when the well is pressurized, which occurs at 5,600s in Figure 4.2.

In Figure 4.2, the test data begins to slowly increase between $t = 0.1$ s and $t = 1$ s, as the first part of the pressure signal reaches the gauge in the lower perforation (Figure 4.3, red line). From 1 to 10s, the test data undergoes a rapid increase in pressure before decreasing abruptly. At around 11 s, there is a jump in the test data followed by a steady increase until the end of the test at 10,000 s. The erratic data during this period is due to the way pressure is applied at the surface by a pump that does not have constant rate control.

The simulated data for each of the three cases are reasonably close to the test data, but no single case can emulate the full test response from early to late time. Cases 1 and 3 compare best to the test data at early time, $t < 1$ s. While Case 2 matches better between 10 s and 100 s. None of the cases compare well with the test data at late time. For all of the simulated cases, the slope in the response curve is less than the test data from 1000 s to 10,000 s.

Discussion

It appears from the VIT analysis that the effective permeability of the zone is close to one of the three simulated cases, though it is difficult to determine which case is the best comparison. The fact that the simulated data does not match perfectly with the test data is to be expected given that the simulated system is only an approximation of the real physical system. Two key assumptions that may contribute to the discrepancy in the simulated results are radial symmetry and homogeneous permeability in the cross-section of the barrier system. In addition, uncertainties in system parameters, such as the shale permeability and compressibility, are also important factors in how well the simulated data is able to match the test data. Given this discussion, the VIT analysis is limited to estimating the effective permeability of the barrier system within an order of magnitude, between 1 and 10 millidarcy. Further investigation is required to reduce uncertainty in the analysis.

The cement core collected from 4528' MD has a matrix permeability of 0.9- μ D and thus the estimated permeability from the VIT data is 3 to 4 orders of magnitude greater than cement core. The enhanced permeability observed in the VIT is likely due to communication at the interfaces and thus the most likely path of any CO₂ migration would be these interfaces.

5. Conclusions

The primary conclusions from this investigation are:

- a. The barrier system in this well provides hydraulic isolation across the caprock based on formation pressure measurements made during this survey. Effective placement of the Portland-fly ash cement system was a key element in the performance of the barrier system to prevent or limit migration along cement interfaces with casing/borehole.
- b. Cement carbonation has been observed in varying degrees in cores from this well. Carbonation of cement increased permeability, porosity and had a mixed effect on capillary properties with a small increase in capillary entry pressure accompanied by an increase in the fraction of pore water displaced. It decreased the compressive strength but the cement still provides an effective barrier. These changes, while not improvements in cement properties, do not result in a significant loss of cement resistance to CO₂ migration.
- c. The casing is in very good condition, consistent with good cement coverage and limited circulation of reservoir fluids along the casing-cement interface.
- d. Cement interfaces with casing and formation appear to be tight and do not have significant calcium carbonate deposition.
- e. The effective permeability of the barrier system including the cement interfaces was evaluated by numerical modelling of the Vertical Interference Test (VIT) data, which is the preferred method to analyze in-situ migration potential. The VIT data analysis indicates the permeability to be 1-10 millidarcies, which is approximately 3 to 4 orders of magnitude greater than the cement core permeability of 1 microdarcy that was taken from the same interval. Although further investigation is required to reduce uncertainty in this analysis, the results indicate that the cement interfaces with casing and/or formation are the primary path for potential CO₂ migration compared to the cement matrix.
- f. Our interpretation of the data suggests that the CO₂ that has caused carbonation of cement and acidification of fluids adjacent to the caprock originated in the CO₂ reservoir (Dakota formation). The alteration could come from either or a combination of CO₂ diffusion into the caprock or by migration along defects (primarily cement-caprock and cement-formation interfaces) within the wellbore system. History matching the survey data and results will be conducted to distinguish between these two alternatives.
- g. Current technologies can be used to determine wellbore barrier condition. Logging results from this survey correlate with the performance measurement of the large scale vertical interference test (VIT) and the small scale cement core properties.
- h. Based on the results of the surveys in this well, conventional cement-fly ash systems can inhibit CO₂ migration even after carbonation of the cement because permeability remains relatively low and capillary resistance relatively high. The cement interfaces with the casing and formation are the areas of greatest concern for barrier system integrity; however these interfaces appear to provide sufficient flow restriction between formations in this well based on the VIT results, the lack of corrosion in the well, and the lack of sustained casing pressure.

Evidence from this investigation suggests that Portland-based cement systems can be used effectively in creating suitable barrier systems for long-term CO₂ storage operations, if good practices are employed during well construction. Examples of required good practices include: centralization of casing and efficient borehole mud removal for cement placement.

Acknowledgements

The authors express their appreciation to the management of Carbon Capture Project Phase 2 member companies for support of this project. CCP2 member companies are: BP Alternative Energy, Chevron, ConocoPhillips, Eni, StatoilHydro, Petrobras, Shell Global Solutions US Inc. and Suncor Energy Inc. The conclusions in this report are those of the authors and are not necessarily the view of the other member companies.

Special thanks to Charles Christopher, BP Alternative Energy, for the guidance in creating this comprehensive program. Special thanks also to Ray Wydrinski, BP America for support with petrophysical analysis. Special thanks also to Andrew Duguid, Ph.D., and Matteo Loizzo of Schlumberger Carbon Services for their support in this project.